

# SOL-GEL SYNTHESIS, CHARACTERIZATION AND ACTIVITIES OF ALUMINA SUPPORTED NANOPARTICLE CuO-NiO-CeO<sub>2</sub> CATALYSTS FOR WATER-GAS-SHIFT (WGS) REACTION

Naidu V. Seetala<sup>1</sup>, Upali Siriwardane<sup>2</sup>, Ramakrishna S. Garudadri<sup>2</sup>, and Johnte Bass<sup>1</sup>

<sup>1</sup>Department of Physics, Grambling State University, LA 71245

<sup>2</sup>Department of Chemistry, Louisiana Tech University, Ruston, LA 71270

## Introduction

Hydrogen is one of the main energy sources available for the future advancement of clean fuel technologies especially for fuel cells. Generation of hydrogen and CO<sub>2</sub> from Water Gas Shift (WGS) reaction mixtures of CO and H<sub>2</sub>O is of interest to many researchers since it allows a large scale production of hydrogen [1, 2]. The main objective of this work is to develop low temperature bimetallic WGS nanocatalysts with higher conversion efficiencies to produce hydrogen from CO and steam mixtures. The catalyst loaded with metal nanoparticles significantly enhances the catalytic activity [3]. Mesoporous materials such as silica or alumina have been used as the high surface area supports for nanocatalysts [4]. Metal oxide nanoparticles incorporated mesoporous support framework could offer size dependent advantages [5] such as least diffusion resistance, easy accessibility to reactants, and large number of active sites. In this paper, the preparation and catalytic activities of alumina granular catalysts incorporating metal oxide nanoparticles using sol-gel/oil-drop methods [6, 7] will be presented.

## Experimental

Sol-gel/oil-drop methods [6, 7] were tailored in our laboratory to prepare alumina-supported metal oxide nanoparticles incorporated WGS catalyst granules. This procedure using precursor aluminum tri-sec butoxide (ALTSB) involves three main steps: 1) boehmite solution preparation, 2) homogenizing metal oxides nanoparticles, promoter and alumina sol in appropriate concentrations, 3) gelation of metal oxide/alumina sols, and 4) sol-gel shaping into spherical granules and hardening them in hot mineral oil. The compositions of Cu and Ni were varied within 10% while Ce and alumina were held at 11% and 79% by weight (wt%), respectively. The resulting granules were filtered, washed with H<sub>2</sub>O/ethanol, and oven dried for two days at 50 °C, and then calcined in a box furnace at 450 °C for 4 hrs. The surface area and pore structure of alumina

granules were analyzed using a NOVA 2000 high-speed gas desorption analyzer employing BET method. A Scintag powder x-ray diffractometer (PXRD) with Ni-filtered Cu-K<sub>α</sub> beam was used to obtain diffraction patterns for samples annealed to various temperatures to study the phase compositions. DTA/TGA analyses were carried out using Shimadzu DTA-50 and TGA-50 for thermal properties.

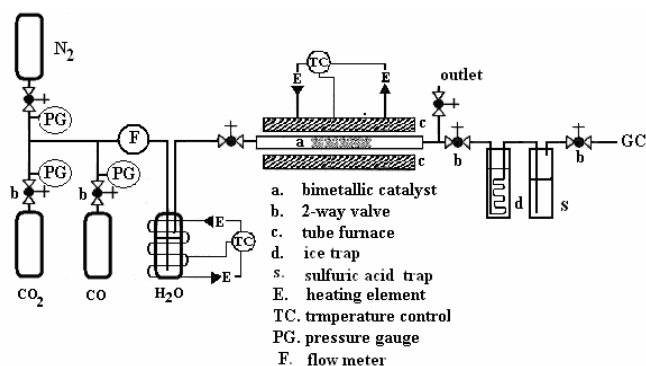


Figure 1: Gas-phase flow reactor for optimizing WGS reaction parameters

A gas phase flow reactor (Figure 1) maintained at 150 to 400 °C with 50 °C temperature increments is used to screen the catalytic activities and obtain optimum reaction temperature of the catalyst. A gas-phase batch reactor (Figure 2) was used to obtain kinetic data from GC injections of product mixtures taken hourly for 13 hours for a catalyst at the optimum WGS reaction temperature to determine the CO conversion and CO<sub>2</sub>

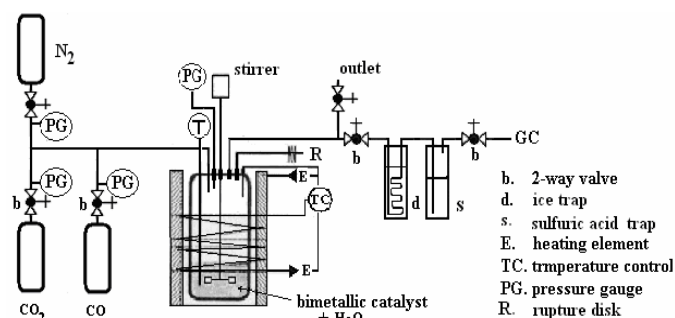


Figure 2: Gas-phase batch reactor for kinetic study of WGS catalysts

production. Both reactors were connected to a HP 8950 series II gas chromatograph (GC) with a Carboxen 1000 (Supelco® Carboxen-1000) column and a thermal conductivity detector (TCD) for product analysis.

## Results and Discussion

DTA and TGA results showed complete dehydration of catalysts by 450°C and the calcination temperature was set at 450 °C. Combined DTA and PXRD analysis indicate that the transition from boehmite to  $\gamma$ -alumina occur at around 250 °C. The BET results tabulated in Table 1 shows that all the catalysts synthesized fall under mesoporous category.

Table 1: BET Surface Area Measurements

Catalyst	Surface area (m <sup>2</sup> /g)	Av. pore size (Å)
Ni(10%)Ce(9%)	401.0 (4.0)	20.57 (0.02)
Ni(10%)Ce(6%)	273.4 (2.7)	20.13 (0.02)
Cu(3%)Ni(7%)Ce(11%)	233.7 (2.3)	15.70 (0.01)
Ni(10%)Ce(11%)	214.8 (2.1)	18.01 (0.01)
Ni(7%)Ce(3%)	211.5 (2.1)	19.79 (0.01)
Ni(10%)	194.6 (1.9)	21.37 (0.02)
Cu(5%)Ni(5%)Ce(11%)	183.7 (1.8)	17.95 (0.01)
Cu(10%)Ce(11%)	156.3 (1.5)	20.11 (0.02)
Cu(7%)Ni(3%)Ce(11%)	141.8 (1.4)	17.97 (0.01)

Figure 3 shows the PXRD spectra for Cu(5%)Ni(5%)Ce(11%)/alumina calcined at 450 °C and further annealed at 1000 °C. No characteristic PXRD peaks for metal oxides (other than alumina support peaks) were observed for samples annealed at 450 °C.

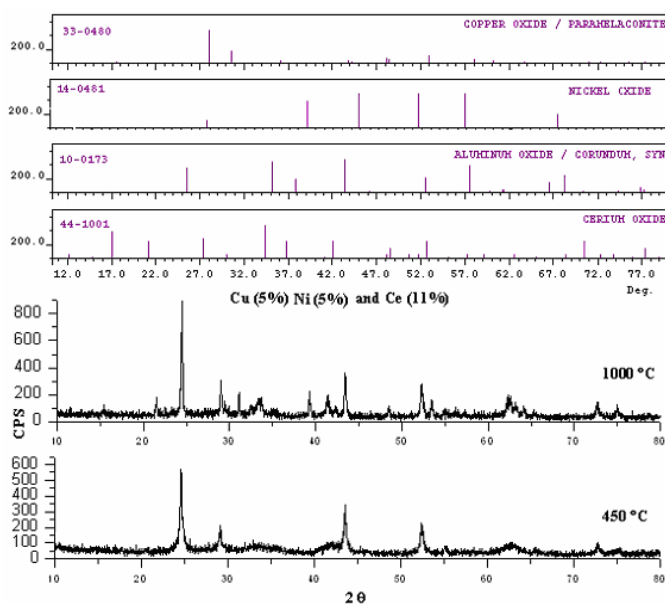


Figure 3: PXRD spectra at 450 °C and 1000 °C for Cu(5%)Ni(5%)Ce(11%)/alumina

Sharper metal oxide PXRD peaks appeared for samples as they were annealed to 1000 °C due to increased crystallinity upon sintering. This is consistent with the nanoparticle nature of the metal oxide nanocrystalline phases that are preserved during the sol-gel synthesis.

Figure 4 shows the gas phase flow reactor results of CO<sub>2</sub> production from WGS reaction for ten catalysts prepared. Since H<sub>2</sub> is difficult to quantify in the GC due to the type of column used and its low sensitivity to TCD, we used the CO<sub>2</sub> molar concentration as direct evidence of WGS reaction taking place. Of the ten catalysts, six catalysts were classified as low temperature shift (LTS) catalysts (150-300 °C) and four as high temperature shift (HTS) catalysts (350-400 °C) based on the optimum temperature of the catalyst. The optimum temperatures for each catalyst were later used in gas phase batch reactor to obtain the reaction kinetics data.

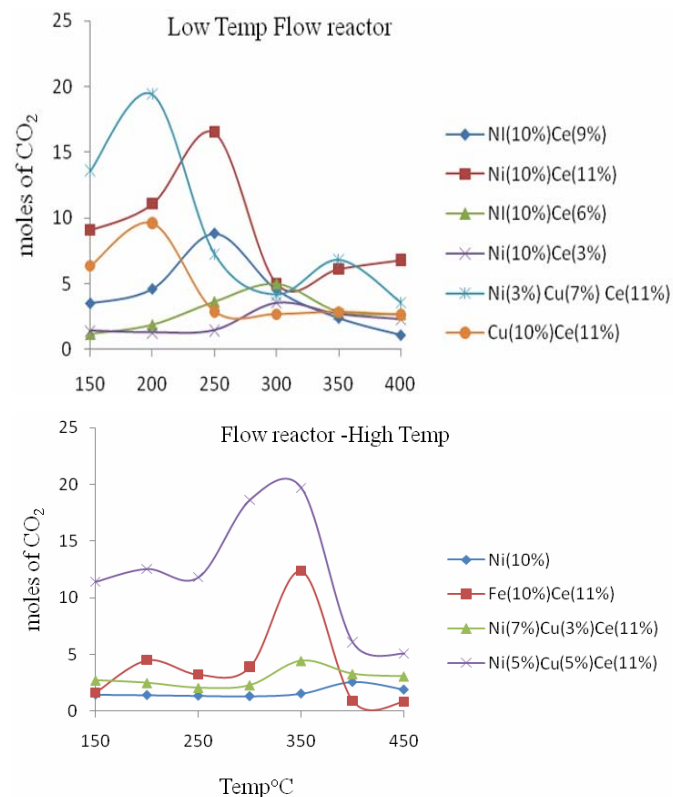


Figure 4: Comparison of gas phase dynamic flow reactor data of LTS and HTS catalysts

Under gas phase flow reactor conditions, Ni(3%)Cu(7%)Ce(11%) LTS catalyst showed the lowest optimum temperature (200 °C) and highest catalytic activity; while among the HTS catalysts studied, Ni(5%)Cu(5%)Ce(11%) showed an optimum temperature of 350 °C and highest catalytic activity.

Figure 5 shows the plots of CO conversion and CO<sub>2</sub> production from batch reactor operated at optimum WGS reaction temperatures for six LTS catalysts. Both the highest initial (1 hr) and final (13 hr) CO conversion was observed for Ni(10%)Ce(3%) followed by Ni(10%)Ce(9%). The highest initial (after 1 hr) CO<sub>2</sub> production was observed for Cu(10%)Ce(11%) catalyst followed by Ni(10%)Ce(9%) and Ni(10%)Ce(11%) catalysts, while the highest final (13 hr) CO<sub>2</sub> production was observed for Ni(10%)Ce(11%) followed by Cu(10%)Ce(11%) and Ni(10%)Ce(9%) catalysts. Though Ni(10%)Ce(3%) showed the highest initial (1 hr) and final (13 hr) CO conversions, it turned out to be one of the lowest initial (1 hr) and final (13 hr) CO<sub>2</sub> production catalyst. This indicates that Ni(10%)Ce(3%) bimetallic composition is a catalyst for different reaction (carbonyl formation, FT etc.) other than water gas shift (WGS) reaction.

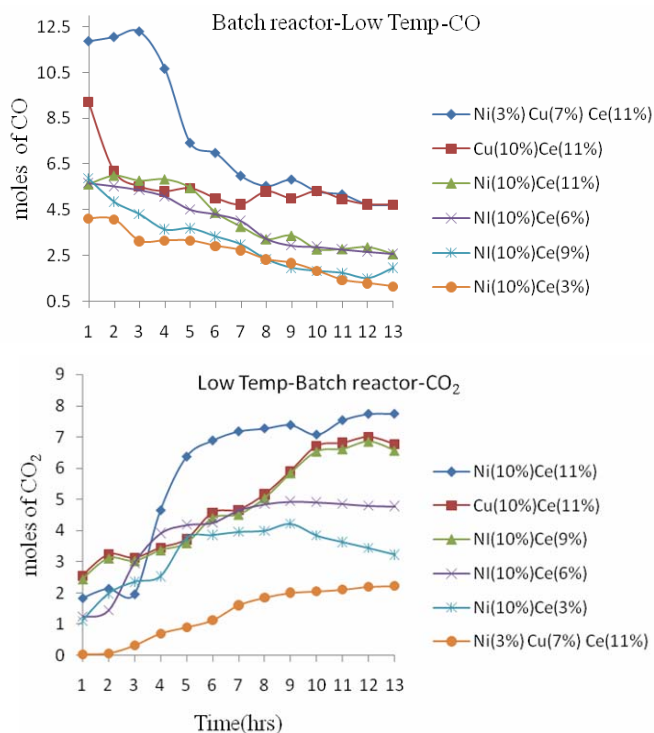


Figure 5: Gas phase batch reactor CO conversion and CO<sub>2</sub> production data of LTS catalysts

Figure 6 shows the plots of CO conversion and CO<sub>2</sub> production from batch reactor at optimum WGS reaction temperatures for four HTS catalysts. Ni(10%) showed the highest initial and final conversions of CO followed by Ni(5%)Cu(5%)Ce(11%) catalyst. But the highest initial and final CO<sub>2</sub> production was observed for Ni(5%)Cu(5%)Ce(11%) catalyst, while Ni(10%) turned out to be one of the lowest CO<sub>2</sub> production catalyst. This indicates that Ni(10%) is not a suitable

catalyst for WGS reaction but it has higher reactivity for different reaction channel other than WGS reaction.

We also studied the promoter effects of Ce (CeO<sub>2</sub>) on WGS reaction at fixed Ni composition; and the effect of various Ni and Cu oxides compositions at constant Ce.

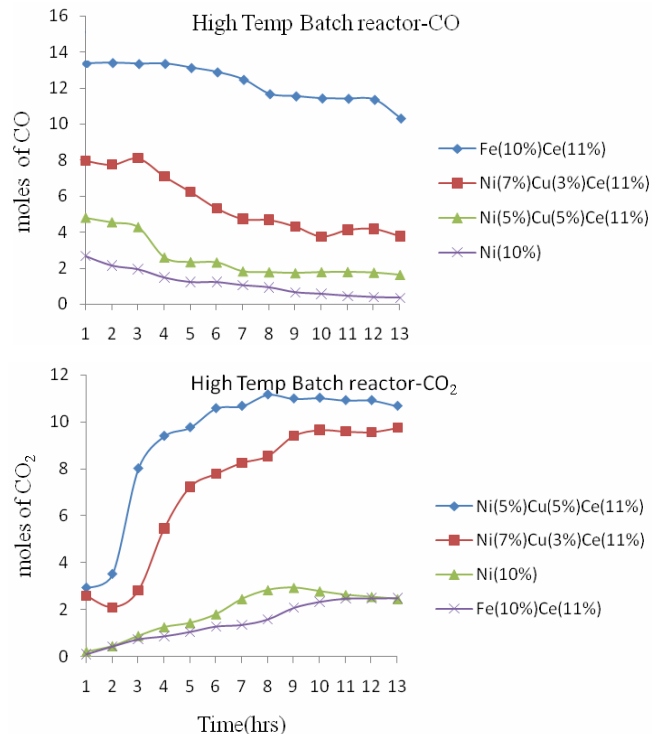


Figure 6: Gas phase batch reactor CO conversion and CO<sub>2</sub> production data of HTS catalysts

Table 2 below shows CO<sub>2</sub> production of several catalysts with constant (Ce composition at 11%) and varying metals (Ni and Cu). Highest production of CO<sub>2</sub> was observed for Ni(5%)Cu(5%)Ce(11%) catalyst at an optimum reaction temperature of 350 °C. Decreasing Ni composition in mixed metal combination of Cu and Ni reduces the catalytic activity.

Table 2: CO<sub>2</sub> Production of Catalysts with Constant Ce Promoter Composition

Catalyst composition	Optimum Temperature (°C)	CO <sub>2</sub> production (% moles) after 13 hr
Ni(5%)Cu(5%)Ce(11%)	350	100.0
Ni(7%)Cu(3%)Ce(11%)	350	90.9
Ni(10%)Ce(11%)	250	71.8
Cu(10%)Ce(11%)	200	61.8
Ni(3%)Cu(7%)Ce(11%)	200	19.9

The effect of various CeO<sub>2</sub> compositions on WGS reaction, with constant Ni composition fixed at 10 wt%,

is shown in Table 3. The best CO<sub>2</sub> production was seen for the Ni(10%)Ce(11%) catalyst with an optimum reaction temperature of 250 °C. Decrease in CeO<sub>2</sub> composition lowered the catalytic activity. It is also observed that a decrease in CeO<sub>2</sub> composition significantly increased the optimum reaction temperature of the catalysts.

Table 3: CO<sub>2</sub> Production of Catalysts with Constant Ni Composition

Catalyst composition	Optimum Temperature (°C)	CO <sub>2</sub> production (% moles) after 13 hr
Ni(10%)Ce(11%)	250	71.8
Ni(10%)Ce(9%)	350	60.0
Ni(10%)Ce(6%)	300	42.7
Ni(10%)Ce(3%)	300	30.0
Ni(10%)	400	17.2

### Conclusions:

The main objective of this work has been accomplished by synthesizing low temperature (LTS) nanocatalysts – Ni(10%)Ce(11%) and high temperature (HTS) nanocatalysts – Cu(5%)Ni(5%)Ce(11%) for Water Gas Shift reaction (WGS) to produce hydrogen from CO and steam mixtures. Sol-gel/oil-drop methods have been successfully modified for the preparation of metal (Cu-Ni-Ce) oxide nanoparticles incorporated alumina granular WGS catalysts: various Cu and Ni metals compositions held at 10%, Ce composition is fixed at 11% and alumina support at 79% by wt%.

The sol-gel synthesized nanocatalysts for WGS were successfully characterized using DTA/TGA analysis, BET techniques for surface area and porosity measurements, and PXRD to confirm metal and alumina support structures. A gas phase flow reactor was successful in screening the catalysts and optimizing reaction temperatures. A gas-phase batch reactor yielded the CO conversion and CO<sub>2</sub> production data. GC analysis of the WGS reaction products from both reactors were successfully used to obtain optimum reaction temperature and kinetic data

DTA and TGA analysis of catalysts showed that dehydration of the granules of metal hydroxides to metal oxides was complete at 450 °C. The surface area of the catalysts were 150- 400 m<sup>2</sup>/gm with an average pore size of 20 Å, confirmed the mesoporous nature of the WGS catalysts. No characteristic PXRD peaks for

metal oxides were observed for samples annealed below 450 °C confirming the nanoparticles nature of the active metal oxides on alumina support, and further annealing to 1000 °C confirmed the presence of various metal oxide phases as PXRD peaks appeared upon sintering of nanocatalysts to higher crystallinity. Our data supports the preservation of nanoparticles of the metal oxide phases during the sol-gel synthesis and upon calcinations at 450 °C of catalysts.

GC data shows that six of the ten catalysts prepared were LTS catalysts with optimum temperatures between 200-300 °C, and other four were HTS catalysts with optimum temperatures between 350-400 °C. Based on catalytic activities, Ni(10%)Ce(11%) catalyst was found to be the best WGS catalyst among the LTS catalysts, while Ni(5%)Cu(5%)Ce(11%) was found to be the best HTS catalysts. The Ce promoter had a significant effect on optimum reaction temperature as well as catalytic activity. Increasing Ce composition had a favorable effect by reducing the optimum WGS reaction temperature and enhancing the catalytic activity. The effect of various Ni compositions at constant Ce was also studied. The lower Ni compositions favored WGS reaction: the CO<sub>2</sub> (hydrogen) production.

### Acknowledgements:

This work is supported by a grant from the Department of Energy (DOE), grant#DE-FG26-07NT43064.

### References

- 1.H.-M. Cheng, H.M. Quan, Yang, L. Chang, "Hydrogen storage in carbon nano tubes," *Carbon*, vol 39, pg 1447-1454, 2001.
- 2.O.Z. Ilse, "Catalytic processes for clean hydrogen production from hydrocarbons," *Turkish Journal of Chemistry*, vol 31, pg 531-550, 2007.
- 3.A. Schwarz, C. Contescu, C. Adriana, "Methods for preparation of catalytic materials," *Chemical Reviews*, vol 95, pg 481-486, 1995.
- 4.S. Sie, Process development: Case history of FT synthesis, *Rev. Chem. Eng.* 1998, 14, 109–157.
- 5.K. Okabe, et al., *Energy & Fuels* 17 (2003) 822.
- 6.J. Hajek, D.Y. Murzin, "Short introduction to sol-gel chemistry in heterogeneous catalysis," *Nanocatalysis*, pg 9-32, 2006.
- 7.Naidu Seetala and Upali Siriwardane, DOE final report 2005, Grant# DE-FG26-00NT40836.